Journal of Mathematics and Statistics 1 (2): 106-112, 2005
ISSN 1546-3644

Analysis of the Chord Length Distribution Along an Edge: The Wedge Case and the Quadratic Rod Case

Wilfried Gille
Department of Physics, Martin-Luther-University Halle-Wittenberg
Hoher Weg 8, D-06120 Halle, Germany

Abstract: The analytic expression is given for the chord length distribution density $f(l,b)$ along the edge of an infinitely long rectangular wedge and for a quadratic rod, both of constant breadth b. The general result is: A constant behaviour for $0 < l < b$ and a finite jump of size $2/b$ at $l = b$ is an intrinsic feature of a rectangular edge.

Key words: IUR Chords, Chord Length Distribution, Pattern Recognition

INTRODUCTION

This article considers a particular problem in geometric probability, the solution of which is useful in pattern recognition of three-dimensional geometric figures.

The automatic recognition of the particle shape of geometric objects on a length scale from the nm-region up to some meters is of immense interest in many fields. Chord length distributions can be obtained experimentally via special procedures from image material [1]. Thus, analytic expressions of chord length distributions possess stereological applications in the field of pattern recognition of geometric figures from digital image analysis [2]. So, particle shape and size can be recognized experimentally. It is useful to approximate more complicated particle shapes by simple geometric figures. This strategy is also particularly useful for those cases, where microparticles cannot be inspected by a microscope or by any other image generating method. For example, this is the case if scattering methods are applied for particle characterization.

A far-reaching particle characterization is possible by the use of smooth particle shape models, considering random chords l with an Isotropic Uniform Random (IUR) orientation in space. Chord length distribution densities $f(l)$ are fingerprints of three-dimensional particles [3].

If a particle possesses sharp edges, (as in the case of a parallelepiped, tetrahedron, triangular rod, quadratic rod or hemisphere), the properties of these edges will be reflected into $f(l)$ for small chord lengths. Based on this behaviour it seems to be useful to establish an "edge - pattern". Such a pattern is defined and analyzed in this study. A straight infinitely long rectangular edge exists in two basic modifications, wedge (Fig. 1) and quadratic rod. The analysis of $f(l)$ will allow for detecting the existence of an edge.

It is well-known that $f(l)$ functions are sensitive indicators of the geometric shape. For example, this was reported by Stoyan *et al.* [4], Enns and Ehlers [5] and Gille [6]. This was a subject of previous articles and textbooks [7-9]. There are connections with more general papers and textbooks [10, 11].

Obviously, the existence of a sharp edge leads to many small chord segments. Consequently, the relation $\lim_{l\to 0} f(l) > 0$ allows a clear distinction between a smooth face possessing no surface singularities (e. g. ellipsoid) and an angular one. In order to study this phenomenon in more detail, the characteristic of $f(l)$ for a pure wedge is investigated in this work, independent of the detailed shape of the whole geometric figure, which this wedge is part of.

Peculiarities of the Chord Length Distribution Along a Wedge: Let l be a random variable, the random chord length, $0 \le l < \infty$, which results whenever a fixed convex body is intersected by an IUR field of straight lines. An IUR chord length distribution $F(l)$ results. The function $F(l)$ and the distribution density $f(l) = F'(l)$ depend on shape and size of the (actual) geometric figure.

For a convex body, the geometric covariogram $K(l)$ and $f(l)$ are connected by

$$f(l) = -\frac{K''(l)}{K'(0)}. \qquad (1)$$

Operating with the geometric covariogram $K(r)$ [7, 12], Eq. (1) has been investigated in more detail by Enns and Ehlers [5].

The diversity of $f(l)$ functions is immense. All details of the shape of a geometric body influence the behaviour of $f(l)$. However, without special

assumptions about the shape of the body, $f(l)$ does not define a geometric object.

The wedge is defined (Fig. 1) by the following: Two planar stripes, each of infinite length and width b, are joined at a right angle to form the shape which resembles an "angle iron". This shape is involved in a wide class of geometric figures. Because an edge is a non-compact and non-convex set, Eq. (1) cannot be applied and the determination has to go back to elementary geometric principles.

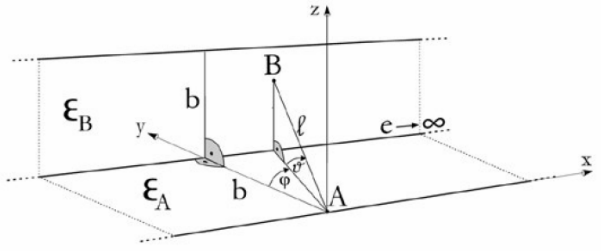

Fig. 1: A Random Line Enters the Wedge at **A,** Travels through the Space between both Planar Stripes and Hits the Boundary again at Point **B.** The Chord Possesses the Length $l=\overline{AB}$ and its Direction in Space is Defined by the Angles φ and ϑ. Because of $e\to\infty$, without any Restriction, the Chord Position along the Wedge is Arbitrary. Without Changing the Angles φ and ϑ, the Points **A** and **B** can be Shifted to any Position along the Wedge

The straight edge considered possesses two modifications: On the one hand, it can be a part of any rectangular solid, especially of a quadratic rod. On the other hand, it can be part of a wedge. However, a wedge is not a trivial special case of a quadratic rod, which represents a compact convex set. The wedge cannot be analyzed via Eq. (1). So it is not a trivial question to investigate differences and common properties of wedge and rod.

Determination of $f_w(l,b)$: A wedge of length e, $e\to\infty$ and breadth b, $0\le b<\infty$, consisting of two stripes in the planes $\in_A$ and $\in_B$, is analyzed. The wedge is in a fixed position in the x-y-z - coordinate system (Fig. 1). The plane $\in_B$ is fixed parallel to the x-z plane and $\in_A$ lies in the x-y plane. Considering a constant chord length l (and all the following considerations require a well-defined constant chord length l), the intersection of the straight line $\overline{AB}$, which stretches between the planes $\in_A$ and $\in_B$, is described by two direction angles φ and ϑ.

The parallel translation of $\overline{AB}$ along the edge ($\varphi=const$ and $\vartheta=const$) does neither change the length l nor the constellation. Thus, it is sufficient to consider one typical chord of length l at a fixed place of the infinitely long wedge. Close connections between l and the position of the points **A**, **B** exist (Appendix). The detailed calculation is based on the definition of the distribution function $F_w(l)$. The following formulas are exclusively related to the one stripe, which lies in $\in_B$. The other one contributes in the same manner.

Based on the spherical polar coordinates adopted for the definition of the direction of the random straight line $\overline{AB}$, the area element on the unit sphere is proportional to $\cos(\vartheta)\cdot d\varphi d\vartheta$. IUR chords require: The random variable ϑ is uniformly distributed in the interval $0\le\varphi\le\pi/2$ and the variable ϑ possesses the distribution density $\cos(\vartheta)$, $0\le\vartheta\le\pi/2$.

However, special restrictions for the variables φ and ϑ have to be introduced, in order to "guarantee" that $\overline{AB}$ does always hit the wedge coming from **A** in the direction (φ,ϑ). Depending on l and b, certain limiting angles have to guarantee the existence of point **B** on the wedge. The surface area $S_{\in_B}=e\cdot b-e\cdot l\cdot\sin(\vartheta)$, which lies in $\in_B$, is a part of the plane $\in_B$ and excludes the existence of chords, which are smaller than l (Fig. 6). Besides the area element of the unit sphere $(2/\pi)\cdot\cos(\vartheta)\cdot d\vartheta d\varphi$, it must be taken into account that the plane $\in_B$ and the chord direction $\overline{AB}$, are not perpendicular to on one another (Fig. 1 and 2). Let $\in_l$ be the plane which is perpendicular to the chord direction and includes the point **B** (Fig. 2). Then, the surface area part, $S_{\in_l}=S_{\in_B}\cdot[\cos(\vartheta)\cdot\cos(\varphi)]=[e\cdot b-e\cdot l\cdot\sin(\vartheta)][\cos(\vartheta)\cdot\cos(\varphi)]$ represents the projection of the surface area $S_{\in_B}$ into the plane$\in_l$.

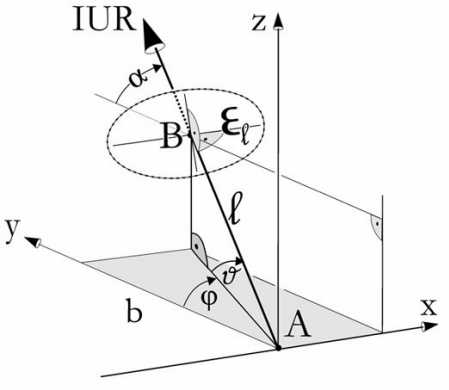

Fig. 2: The Plane $\in_l$, Passing through the Point **B**, is Perpendicular to the Chord Direction and α is the Angle between the Planes $\in_l$ and $\in_B$

The factor $[\cos(\vartheta)\cdot\cos(\varphi)]$ can be verified in greater detail (Fig. 2): Point **B** possesses the coordinates $x_B = l\cdot\sin(\varphi)\cos(\vartheta)$, $y_B = l\cdot\cos(\varphi)\cos(\vartheta)$, $z_B = l\cdot\sin(\vartheta)$. Consequently, the plane $\in_l$ is given by $x_B\cdot x + y_B\cdot y + z_B\cdot z - l^2 = 0$. The plane $\in_B$ is $y\cdot b - b^2 = 0$. The angle between $\in_l$ and $\in_B$ is denoted by α. Consequently, $S_{\in_l} = S_{\in_B}\cdot\cos(\alpha)$. The term $\cos(\alpha)$ results from the scalar product of the orientation vectors of the planes $\in_l$ and $\in_B$, $\cos(\alpha) = y_B\cdot b/(l\cdot b) = \cos(\varphi)\cdot\cos(\vartheta)$.

Thus, $S_{\in_l} = S_{\in_B}\cdot\cos(\alpha)$.

Exclusively in the limiting case $\varphi = \vartheta = 0$ the factor $\cos(\alpha)$ equals unity. In all other cases, the whole term $[e\cdot b - e\cdot l\cdot\sin(\vartheta)]\cdot[\cos(\vartheta)\cdot\cos(\varphi)]$ has to be considered.

Altogether, the analysis of the ratio of the measure of *favourable cases* to the measure *of cases possible at all* for the wedge yields

$$F_w(l) = 1 - \frac{\sum_i\left\{\int_{\varphi_i}\int_{\vartheta_i}[e\cdot b - e\cdot l\cdot\sin(\vartheta)]\cdot[\cos(\vartheta)\cdot\cos(\varphi)]\cdot\cos(\vartheta)\frac{2}{\pi}d\vartheta d\varphi\right\}}{\int_0^{\pi/2}\int_0^{\pi/2} e\cdot b\cdot[\cos(\vartheta)\cdot\cos(\varphi)]\cdot\cos(\vartheta)\frac{2}{\pi}d\vartheta d\varphi} \quad (2)$$

The denominator does not depend on l. The denominator term $e\cdot b\cdot[\cos(\vartheta)\cdot\cos(\varphi)]$ represents the projection of the whole surface area $e\cdot b$ (the whole upper part of the wedge, which lies in the plane $\in_B$) into the direction perpendicular to the chord direction (φ,ϑ). It is averaged by the factor $\cos(\vartheta)\cdot(2/\pi)\cdot d\vartheta d\varphi$. For the measure of the *cases possible at all*, the restrictions of the integration limits are given by the all-including integration limits, $0\le\varphi\le\pi/2,\ 0\le\vartheta\le\pi/2$.

Based on a constant length l, the numerator term in Eq. (2) involves a sum of several integration regions, defined by certain integration limits ϑ_i and φ_i, depending on l and b. This is explained in the Appendix, starting from the simple "angle-case" in R^2, followed by the case of the so-called "one side infinity wedge" in R^3 ending in the wedge case.

At first, the analysis of the geometric constellation requires an interval splitting of the chord length l as depending on b. In the wedge case, three different l-intervals, I1: $\{0\le l\le b\}$, I2: $\{b\le l\le\sqrt{2}\cdot b\}$, I3: $\{\sqrt{2}\cdot b\le l\le\infty\}$ have to be selected. In these intervals the integration limits vary in terms of l, b and of the sum index i. In more detail, in the intervals I1, I2, I3, the sum terms in Eq. (2) are given by a sequence of definite integrals.

The integrand is given by the abbreviation g, $g = (e,b,l,\vartheta,\varphi) = [e\cdot b - e\cdot l\cdot\sin(\vartheta)]\cdot[\cos(\vartheta)\cdot\cos(\varphi)]\cdot\cos(\vartheta)\frac{2}{\pi}$.

I1: For $i=1$; There are exclusively the all-including integration restrictions $\{0\le\varphi\le\pi/2\}$, $\{0\le\vartheta\le\pi/2\}$

Consequently the sum reduces to the one term $\int_{\varphi=0}^{\pi/2}\int_{\vartheta=0}^{\pi/2} g\,d\vartheta d\varphi$.

I2: Here, two cases, $i=1$; $\{0\le\varphi\le\arccos(b/l),\ \arccos(b/(l\cdot\cos(\varphi)))\le\vartheta\le\arcsin(b/l)\}$ and $i=2$; $\{\arccos(b/l)\le\varphi\le\pi/2,\ 0\le\vartheta\le\arcsin(b/l)\}$ must be selected,

$$\int_{\varphi=0}^{\arccos(b/l)}\int_{\vartheta=\arccos(b/(l\cdot\cos(\varphi)))}^{\arcsin(b/l)} g\,d\vartheta d\varphi + \int_{\varphi=\arccos(b/l)}^{\pi/2}\int_{\vartheta=0}^{\arcsin(b/l)} g\,d\vartheta d\varphi .$$

I3: Here, two cases, $i=1$; $\{\arccos(b/\sqrt{l^2-b^2})\le\varphi\le\arccos(b/l),\ \arccos(b/(l\cdot\cos(\varphi)))\le\vartheta\le\arcsin(b/l)\}$ and $i=2$; $\arccos(b/l)\le\varphi\le\pi/2,\ 0\le\vartheta\le\arcsin(b/l)\}$result,

$$\int_{\varphi=\arccos(b/\sqrt{l^2-b^2})}^{\arccos(b/l)}\int_{\vartheta=\arccos(b/(l\cdot\cos(\varphi)))}^{\arcsin(b/l)} g\,d\vartheta d\varphi + \int_{\varphi=\arccos(b/l)}^{\pi/2}\int_{\vartheta=0}^{\arcsin(b/l)} g\,d\vartheta d\varphi .$$

Operating with the terms I1 and I3, the properties $F_w(0,b)=0$ and $F_w(\infty,b)=1$ can be confirmed.

The chord length distribution density $f_w(l,b)$: Integration of Eq. (2), followed by one differentiation step with respect to l, yields analytic expressions at the intervals I1, I2 and I3. The detailed calculation for I2 and for I3 is elaborate. It includes features similar to the case of the parallelepiped [13, 14]. The result is

$$f_w(l,b) = \begin{cases} I1: & \dfrac{4}{3\pi b} \\ I2: & \dfrac{6\pi b^3 + 4l^3 - (4b^2+8l^2)\sqrt{l^2-b^2}}{3\pi b l^3} \\ I3: & \dfrac{4}{3\pi b l^3}(l^3 + (b^2+l^2)\sqrt{l^2-2b^2} - (b^2+2l^2)\sqrt{l^2-b^2} + 3b^3\cdot\arctan(\dfrac{b}{\sqrt{l^2-2b^2}})) \end{cases} \quad (3)$$

No abbreviation is used in Eq. (3). Most of the terms do not simplify before the very last step of the calculation

project, $g_w(l) = F_w'(l)$. Connections, given by Camko *et al.* [15].

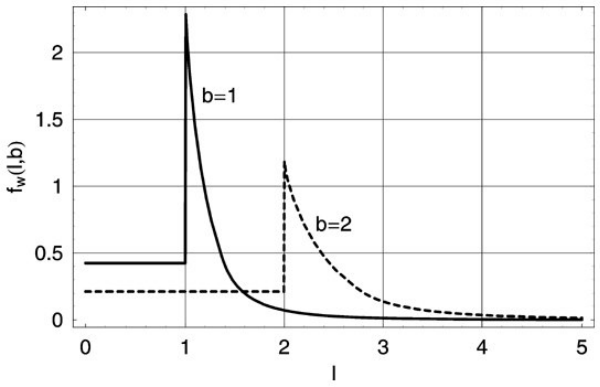

Fig. 3: IUR Chord Length Distribution Density $f_w(l)$, $0 \le l \le 5$, for Fixed b (two cases). In the Limiting Case $b \to 0$, $A(l) = 2 \cdot \delta(l-0)$ Results. The Wider the Wedge the Smaller $f_w(0,b)$

Deciding features of the behaviour of $f_w(l,b)$ (Fig. 3) are:

The function possesses the constant value $4/(3\pi b)$ in I1. The spike of height $f_w(b+,b) = (4+6\pi)/(3\pi b)$ significantly marks b. The finite jump at $l = b$ equals $2/b$. The first moment of $f_w(l,b)$ is $M_1 = b$. Even in the case of a superposition $f_{w12}(l) = c_1 \cdot f_{w1}(l,b_1) + c_2 \cdot f_{w2}(l,b_2)$, $f_{w12}(l)$ remains a constant function if $l < Min(b_1,b_2)$.

The behaviour of f_w for large chord lengths can be studied via the series development of $f_w(l)$ $(b = const)$ at $l \to \infty$. Considering $f_w(l,b)$ in the interval I3 (Eq. 3), the first four terms of the asymptotic expansion of $f_{w\infty}(l,b)$ (the function $f_w(l,b)$ for large l, $l \to \infty$) are

$$f_{w\infty}(l,b) = \frac{1}{\pi b} \cdot \left\{ 3 \cdot \left(\frac{b}{l}\right)^4 + \frac{5}{3} \cdot \left(\frac{b}{l}\right)^6 + \frac{119}{80} \cdot \left(\frac{b}{l}\right)^8 + \frac{87}{56} \cdot \left(\frac{b}{l}\right)^{10} + O\left[\left(\frac{b}{l}\right)^{11}\right] \right\}. \quad (4)$$

The smaller the ratio b/l, the better $f_{w\infty}$, given by Eq. 4, approximates f_w.

Extrapolating $f_{w\infty}(l,b)$ back to $l = b$, an approximation $f_{wa}(l,b)$ for $f_w(l,b)$ at $0 \le l < \infty$ is obtained:

$\{I1: f_{wa}(l,b) = 4/(3\pi b);\ I2 \text{ and } I3: f_{wa}(l,b) = f_{w\infty}(l,b)\}$

Operating with three terms of $f_{w\infty}(l,d)$, (Eq. 4), $f_{wa}(b,b) \approx 2.453/b$ holds.

Considering a finite edge length e, for example $e = 10 \cdot b$ (see the special case of the rectangular bar, Gille [13]), a modified distribution density is obtained. However, a linear decreasing behaviour for small chords exists. This *property of linearity* holds true for the tetrahedron as well.

Moreover, the common properties of the "pure" wedge, just considered, and the wedge as part of a rectangular solid, are much farther reaching. This will be touched in the following section.

Wedge and Quadratic Rod: Now, the wedge chord length distribution density, Eq. (3), is compared with that of an infinitely long quadratic rod of edge b, $f_r(r,b)$. Hereby, the function f_r is a special case of the density obtained for the infinitely long rectangular rod with edges a, b, $0 < a \le b$. Further, the rectangular rod case has been traced back to that of the general rectangular solid with edges a, b, c, $0 \le a \le b \le c < \infty$, [13].

The function $f_r(r,b)$ is

$$f_r(r,b) = \begin{cases} \dfrac{4}{3\pi b}, & \text{if} \quad 0 \le r < b \\ T_2(r,b), & \text{if} \quad b \le r < \sqrt{2} \cdot b \\ T_3(r,b), & \text{if} \quad \sqrt{2} \cdot b \le r < \infty \end{cases},$$

$$T_2(r,b) = \frac{2}{\pi b}\left(\frac{2}{3} + \frac{3b^3\pi - 2\sqrt{r^2-b^2}\,(b^2+2r^2)}{3r^3}\right), \quad (5)$$

$$T_3(r,b) = \frac{2}{3\pi b r^3}(3\pi b^3 + 2r^3 + 2\sqrt{r^2-2b^2}\,(b^2+r^2) - 2\sqrt{r^2-b^2}\,(b^2+2r^2) - 6b^3 \arctan(\sqrt{r^2-2b^2}/b))$$

Considering the term $T_3(r,b)$ (last r-interval, $\sqrt{2} \cdot b \le r < \infty$), the first terms of the asymptotic development of $f_r(r,b)$ are

$$f_{r\infty}(r,b) = \frac{3b^3}{\pi r^4} + \frac{5b^5}{3\pi r^6} + \frac{119b^7}{80\pi r^8} + O\left|\left(\frac{1}{r}\right)^9\right|. \quad (6)$$

The leading asymptotic term equals $3b^3/(\pi r^4)$, compare with Eq. (4).

In addition to the wedge, this figure possesses two times two *parallel* faces. The corresponding chord lengths between them, of course, also are reflected into the chord length distribution.

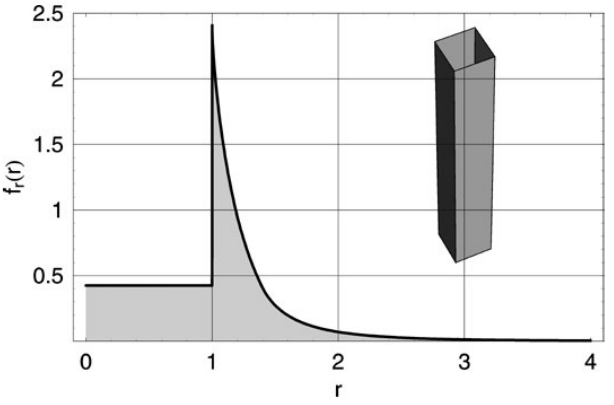

Fig. 4: Chord Length Distribution Density $f_r(r) = f(r,b)$ of an Infinitely Long Quadratic Rod with b=1

For the quadratic rod, $f_r(r,b) = 4/(3\pi b)$, if $0 \le r < b$, is obtained, followed by a finite jump of size $2/b$ at $r = b$. Indeed, there is no difference in the size of the finite jump at $r = b$. The functions f_r and f_w agree in the interval $0 \le r \le b$.

Furthermore, a comparison of Fig. 3 and 4 makes clear that the functions $f_r(r,b)$ and $f_w(r,b)$ are very similar for $b < r < \infty$, too. The leading asymptotic terms agree. In fact, the simultaneous existence of the finite jump at $r = b$ *and* of the size $2/b$ of this finite jump *and* the agreement of the leading asymptotic terms (no differences between Eqs. 4, 6) are a characteristic feature of a wedge and of a rod.

CONCLUSION

In the present study the function $f_w(l,b)$ for an infinitely long wedge of breadth b is added to the set of known functions.

The new density $f_w(l,b)$ calculated, (Eq. 3) and plotted (Fig. 3) is a fingerprint, useful for automatic shape recognition of long rectangular edges. As expected, the analytic expression is not simple, see also the remarks about such projects by Gille [14]. Nevertheless, Eq. (3) involves an uncomplicated, but profound property, very useful for the identification of an edge in practice:

The existence of a finite jump in a function $f(l)$ at a certain abscissa $l = b$ is a hint for the existence of a rectangular edge of width b. Moreover, finding a jump of size $2/b$ between the lower level $\{l \to b-, f(b-,b)\}$ and the peak coordinate $\{l \to b+, f(b+,b)\}$ is a deciding hint that an edge was detected. By this way, an automatic procedure can be established to identify the width b. Moreover, the asymptotic development Eq. (4) allows to estimate the parameter b, too.

In fact, the assumption of a rectangular wedge is a special case. In the future it should be possible to analyze the general wedge more systematically, considering other fixed wedge angles α, $0 < \alpha < \pi$, $\alpha = \pi/n$, $n = 3,4,5...)$. The triangular rod $(\alpha = \pi/3)$ has been investigated [16].

Appendix

In order to be prepared for investigating the interval splitting in the wedge case, Eq. (2) and (Fig. 1), it is instructive to start in R^2 with the limiting case of the right angle (side length b), followed by the analysis of the "one side infinity" wedge (Fig. 6).

The limiting case $\varphi \equiv 0$ yields a plane figure, the right angle, where each side equals b, in the y-z plane, see Fig. 1. Here, the direction angle ϑ is evenly distributed in $0 \le \vartheta \le \pi/2$. The largest chord length is $\sqrt{2}b$. Two l intervals, I1: $\{0 \le l \le b\}$ and I2: $\{b \le l \le \sqrt{2} \cdot b\}$, have to be distinguished, whereas for I2 the ϑ-limits $\arccos(b/l) \le \vartheta \le \arcsin(b/l)$ result. Altogether, the distribution function $F_a(l,b)$ of the random chord length l is defined by

I1: $$F_a(l,b) = 1 - \int_{\vartheta=0}^{\pi/2}[b - l \cdot \sin(\vartheta)] \cdot \cos(\vartheta) d\vartheta \Big/ \int_{\vartheta=0}^{\pi/2} b \cdot \cos(\vartheta) d\vartheta$$

I2: $$F_a(l,b) = 1 - \int_{\vartheta=\arccos(b/l)}^{\arcsin(b/l)}[b - l \cdot \sin(\vartheta)] \cdot \cos(\vartheta) d\vartheta \Big/ \int_{\vartheta=0}^{\pi/2} b \cdot \cos(\vartheta) d\vartheta$$

The factor $\cos(\vartheta)$ transforms the length $[b - l \cdot \sin(\theta)]$ into a direction, which is perpendicular to that of the chord. The resulting distribution density $f_a(l) = F_a'(l)$ possesses a pole at $l = b$ (Fig. 5),

$$f_a(l,b) = \begin{cases} 0 \le l \le b: & \dfrac{1}{2b} \\ b \le l < \sqrt{2}b: & \dfrac{b^2}{l^2 \cdot \sqrt{l^2 - b^2}} - \dfrac{1}{2b} \\ b < l: & 0 \end{cases} \qquad (7)$$

From the analytic representation, Eq. (7), the first moment $\pi b/4$ results.

The one side infinity wedge (Fig. 6) possesses an infinite length on one side. In agreement with the right-angle-case just considered, the maximum angle ϑ possible for any fixed l, ϑ_{max}, does not depend on φ. If $0 \le l \le b$, then $\vartheta_{max} = \pi/2$, whatever the chord direction is. If $b \le l < \infty$, then $\vartheta_{max} = \arcsin(b/l)$. The φ integration limits do not depend on l. Always

$0 \le \varphi \le \pi/2$ holds true. The marked area, $[e \cdot b - e \cdot l \cdot \sin(\vartheta)]$, excludes chord lengths smaller than l. Two l intervals, I1: $\{0 \le l < b\}$ and I2: $\{b \le l \le \infty\}$, have to be distinguished.

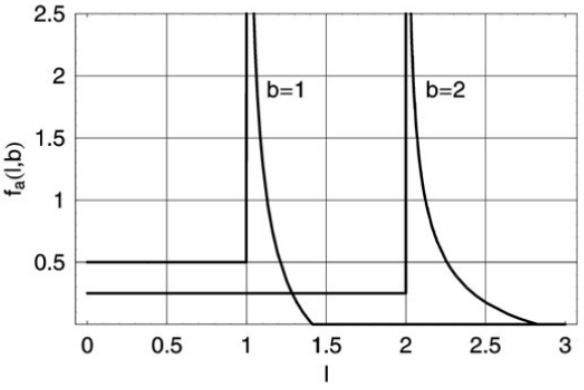

Fig. 5: The Chord Length Distribution Density of the Right Angle in Cases $b = 1$ and $b = 2$

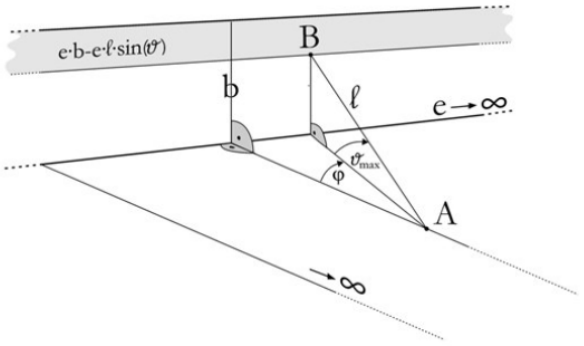

Fig. 6: The "One Side Infinity" Wedge

The formal calculation yields the chord length distribution density of the "one side infinity" edge $f_o(l,b)$,

$$f_o(l,b) = \begin{cases} 0 \le l \le b: & \dfrac{4}{3\pi b} \\ b \le l \le \infty & \dfrac{4(l^3 + \sqrt{l^2 - b^2} \cdot (b^2 - l^2))}{3\pi b l^3} \end{cases}, \qquad (8)$$

which is plotted in Fig. 7. The first moment of $f_0(l,b)$ does not exist.

In the previous two cases (right angle and "one side infinity wedge") the integration regions in the first l interval, $0 \le l < b$, are trivial. Here, the angles ϑ and φ are independent of each other without restrictions. This remains true for the wedge. However, the complete analysis of the wedge of breadth b (Fig. 1 and 8) is a more complicated matter. The reason is: Here, for all $b < l$ the position of point **A** is not free (Fig. 6), but strictly fixed to be on the x-axis of the coordinate system (limiting line of the lower plane $\in_A$). The geometric constellation for determining the limiting angles is analyzed in Fig. 8.

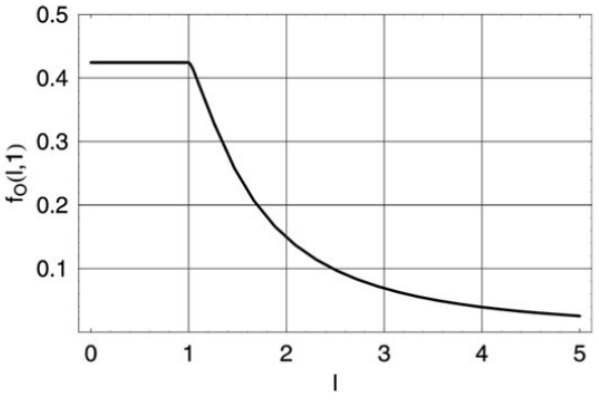

Fig. 7: Distribution Density $f_0(l,b)$ of the "One Side Infinity" Wedge with $b = 1$

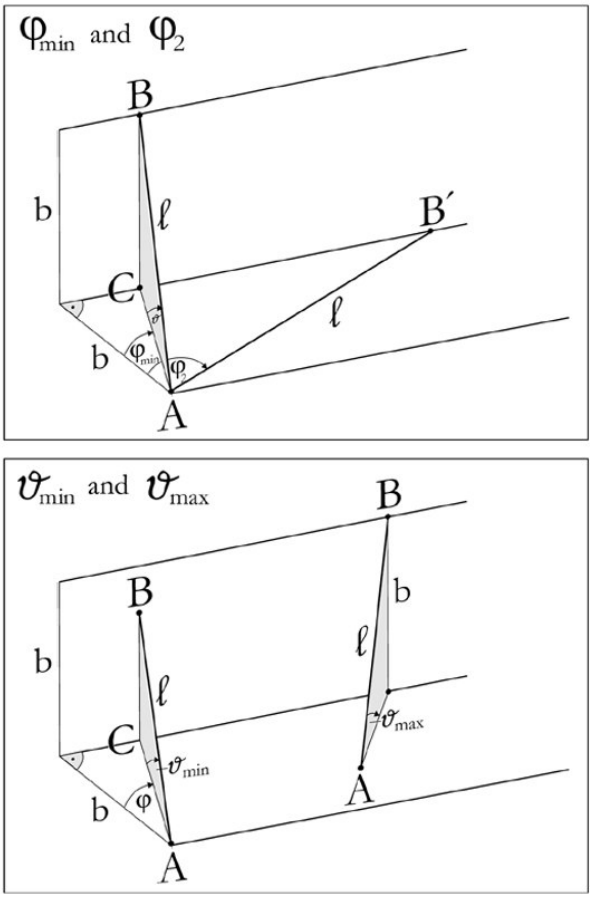

Fig. 8: Analysis of Limiting Angles as Depending on a Constant l for $b \le l$
Upper Part: The Angles φ_{min} and φ_2
Lower Part: The Angles ϑ_{min} and ϑ_2

For I1 there are no additional restrictions for the angles φ and ϑ. However, for I2 the splitting $0 \le \varphi \le \arccos(b/l) \le \pi/2$ must be considered. Depending on these two φ-intervals, there exists the corresponding ϑ interval splitting, $\vartheta_{\min} = \arccos(b/(l \cdot \cos(\varphi))) \le \vartheta \le \arcsin(b/l) = \vartheta_{\max}$ and $0 \le \vartheta \le \vartheta_{\max}$.

In I3, the configuration $\varphi = 0$ represents a limiting case. A lower integration limit $\varphi_{\min}$ exists, which can be studied operating in a triangle **ABC**.

Here, the distance $AC = b/(\cos(\varphi_{\min}))$, consequently $\varphi_{\min} = \arccos(b/\sqrt{l^2 - b^2}$. In the special case $l = \sqrt{2} \cdot b$, $\varphi_{\min} = \arccos(b/\sqrt{2b^2 - b^2} = 0$. The maximum angle $\varphi = \varphi_2$ results, if $AB' = l$. It is $\varphi_2 = \arccos(b/l)$. In this case $\vartheta \equiv 0$ and the chord l is a line lying in the lower plane of the wedge. There is the restriction $\vartheta_{\min} \le \vartheta \le \vartheta_{\max}$, see both triangles in the lower part of Fig. 8. In order to determine $\vartheta_{\min}$, it follows from the triangle **ABC**, $AC = b/\cos(\varphi)$.

Thus, $\vartheta_{\min} = \arccos\left(\overline{AC}/l\right) = \arccos(b/(l \cdot \cos(\varphi)))$. On the other hand, the limiting angle $\vartheta_{\max}$ does not depend on φ, $\vartheta_{\max} = \arcsin(b/l)$.

REFERENCES

1. Hansen, M.B. and W. Zwete, 2002. Nonparametric estimation of the chord length distribution. Laboratory Report, Department of Mathematical Sciences, Aalborg University, Denmark, pp: 28.
2. Gille, W., 2205. Chord length distributions of the hemisphere. J. Math. & Stat., 1: 24-28.
3. Naumovich, N.V. and T.I. Kriskovets, 1982. Influence of the body shape of the profile of chord length distribution. Acta Stereologica, Proceedings of the 3rd. Eur. Symp. Stereol. 2nd. Part, pp: 51-59.
4. Stoyan, D., W.S. Kendall and J. Mecke, 1987. Stochastic Geometry and Its Applications. New York: J. Wiley.
5. Enns, E. and P. Ehlers, 1978. Random paths through a convex region. JAP, 15: 144-152.
6. Gille, W., 2000. Analysis of the chord length distribution of the right circular cone for small chord length. Computers and Mathematics with Applications, 40: 1027-1035.
7. Matheron, G., 1975. Random Sets and Integral Geometry. New York/London: J. Wiley and Sons.
8. Serra, J., 1982. Image Analysis and Mathematical Morphology. London: Academic Press.
9. Feigin, L.A. and D.I. Svergun, 1987. Structure Analysis by Small-angle X-ray and Neutron Scattering. New York: Plenum Press.
10. Aubert, A. and D. Jeulin, 2000. Estimation of the influence of second and third order moments on random sets reconstructions. Pattern Recogn. 33: 1083-1103.
11. Torquato, S., 2002. Random Heterogeneous Materials- Microstructure and Macroscopic Properties. New York: Springer.
12. Nagel, W., 1990. Das geometrische Kovariogram und verwandte Größen zweiter Ordnung, Habilitationsarbeit, Friedrich-Schiller-Universität, Jena.
13. Gille, W., 1988. The chord length distribution density of parallelepipeds with their limiting cases. Exp. Techn. d. Physik, 36: 197-208.
14. Gille, W., 1999. The small-angle scattering correlation function of the cuboid. J. Applied Crystallography, 32: 1100-1104.
15. Camko, C.G., A. Kulbac and O. Maritschew, 1987. Integrali i proiswodnyje drobnowo porjadka i nekotoryje ich priloschenija. (in Russian language), Minsk: Nauka i Technika.
16. Gille, W., 2001. The chord length distribution of a triangular rod. Computational Materials Sci., 22: 151-154.